Polymer 50 (2009) 2981–2989

Contents lists available at ScienceDirect

Polymer

journal homepage: www.elsevier.com/locate/polymer

Application of FTIR spectroscopy to determine transport properties and water–polymer interactions in polypropylene (PP)/poly(ethylene-co-vinyl alcohol) (EVOH) blend films: Effect of poly(ethylene-co-vinyl alcohol) content and water activity

Aurora Lasagabáster [a], María José Abad [b], Luis Barral [b,*], Ana Ares [b], Rebeca Bouza [b]

[a] Departamento de Química Orgánica I, Escuela de Optica, Universidad Complutense de Madrid (UCM), Arcos de Jalón s/n, 28037 Madrid, Spain
[b] Grupo de Polímeros, Departamento de Física, E.U.P. Ferrol, Universidad de A Coruña, Avda. 19 febrero s/n, 15405 Ferrol, Spain

ARTICLE INFO

Article history:
Received 23 September 2008
Received in revised form
1 April 2009
Accepted 3 April 2009
Available online 12 April 2009

Keywords:
FTIR
PP/EVOH blends
Water sorption

ABSTRACT

This paper reports the use of FTIR spectroscopy along with gravimetric analysis to simultaneously study water sorption, transport properties and water–polymer interactions in PP/EVOH films at 25 °C, as a function of EVOH content and water vapour activity. The results indicate the existence of two different mechanisms, below (dual-mode) and above a critical concentration value close to the clustering limit activity. Several spectroscopically distinguishable "types" of sorbed water molecules with different diffusion rates have been detected, and their evolution as a function of the penetrant concentration followed. The main changes in the water structure take place from the clustering limit activity onwards. Significant differences both in the state of water and diffusion sequence of free/bound water have been found between 90/10 PP/EVOH films and blends with EVOH content ≥20%, suggesting not only composite-dependence but also morphology-dependence.

1. Introduction

One of the limiting properties of polymeric materials in food packaging field is their inherent permeability to low molecular weight substances, i.e. gases, moisture and organic vapours. Despite the existence of excellent high barrier materials to gases in oxygen-sensitive food packaging applications, including ethylene–vinyl alcohol copolymers (EVOH), polyamides or polyesters, some of these materials are, for instance, easily plasticized by moisture or do not thermoseal well; consequently, they are more commonly blended with hydrophobic polymers like, polypropylene or polyethylene, or encapsulated in multilayer structures between these hydrophobic polymers [1]. The sorption and diffusion properties of EVOH copolymers and its polypropylene blends are, therefore, of considerable interest from both a fundamental and practical point of view.

The first studies describing water transport properties of EVOH copolymers as a function of ethylene content and temperature have been carried out using gravimetric and the usual plasticization analysis methods [2,3]. In this context, vibrational spectroscopy has proved to be an excellent tool to fully characterize polymer-penetrant transport properties and its associated phenomena, as it is possible to obtain sorption and diffusion parameters and information about polymer-penetrant interactions from the same experiment [4]. It is also relatively straight forward to simultaneously obtain information related to the polymer membrane such as changes in morphology and sorption induced swelling [1,5].

Notwithstanding the relatively high number of publications studying the barrier properties of EVOH copolymers with different ethylene contents using the FTIR technique [4,6,7], there is little cited literature pertaining to polypropylene (PP)/ethylene alcohol vinyl (EVOH) blends. Initial work, concerning the structure of water sorbed in PP/EVOH films as a function of blend composition and the state of water (gaseous or liquid) contacting with the system at equilibrium, high water activity and 25 °C, has previously been published [8]. In addition, the oxygen and water vapour permeation have been studied by directly measuring the oxygen and water vapour transmission rates (O_2TR and WVTR, direct permeation methods) [9,10].

However, to our knowledge the infrared technique has not yet been applied to calculate barrier properties through the PP/EVOH binary blends. In this paper, we present first results on the use of FTIR spectroscopy in transmission to assess the sorption and diffusion process of water through polypropylene (PP)/ethylene alcohol vinyl (EVOH) blends of increasing EVOH content and to

* Corresponding author. Tel.: +349 81337400; fax: +349 81337401.
E-mail address: labpolim@udc.es (L. Barral).

0032-3861/$ – see front matter © 2009 Elsevier Ltd. All rights reserved.
doi:10.1016/j.polymer.2009.04.005

characterize the water–polymer interactions in order to understand the mechanism of water hydration and its possible effects on physical and transport properties.

2. Experimental part

2.1. Materials

An extrusion grade of poly(propylene) (PP) was synthesized by Repsol (ISPLEN PP044W3f). Its melt flow index (MFI) value is of 3.02 g/10 min (230 °C, 2160 g) and density 0.90 g cm^{-3}. The ethylene–vinyl alcohol copolymer (EVOH) from EVAL Europe (grade: F101B) has an ethylene content of 32.9%, an MFI of 1.51 g/10 min (190 °C, 2160 g) and density equal to 1.19 g cm^{-3}.

PP/EVOH blends of increasing EVOH content and compression-molded films for FTIR measurements were prepared according to the procedures described in a previous paper by the authors [8]. All the experiments were carried out in triplicate to check reproducibility and estimate errors. The average thickness of each sample was calculated by micrometer measurement (MarCator 1080, Mahr) at different locations ($n = 100$).

2.2. Experimental procedures

2.2.1. Characterization of PP/EVOH blends

Electron micrographs of gold plated fracture surfaces of the blends were taken with a Jeol JSK-6400 scanning electron microscope (SEM) and published in a previous work [8]. The density of blends was measured in distilled water by Archimede's principle with a density kit of Sartorious LA23OS balance. The void volume fractions were determined by using their measured densities [11] and Eqs. (1) and (2).

$$D_{c,t} = \Sigma M_l/(\Sigma M_i/d_i) = (M_1 + M_2)/(M_1/d_1 + M_2/d_2) \quad (1)$$

where $D_{c,t}$ is the theoretical density of the binary blend, $d_1 = 1.179$ g/cm^3 and $d_2 = 0.899$ g/cm^3 the densities of EVOH and polypropylene, respectively.

$$d_{c,e} = (1 - \varepsilon)d_{c,t} \quad (2)$$

where $d_{c,e}$ is the experimental density of the blend and ε the void volume fraction of the blend film [12].

The degree of crystallinity within each phase was estimated from the FTIR spectra of the dried samples performed in the transmission mode in an OPUS/IR PS15 spectrometer (Bruker). The peak area ratio $A_{998\ cm^{-1}}/A_{973\ cm^{-1}}$ is one of the most common IR band combinations used to estimate the degree of crystallinity of iPP as a function of both material and processing parameters [13]. Besides, the absorbance ratio $A_{1145\ cm^{-1}}/A_{1096\ cm^{-1}}$ is used to estimate the degree of crystallinity of poly(vinyl alcohol) [14].

2.2.2. Water sorption

Film samples were dried at 80 °C for at least 24 h in a vacuum oven (20 Pa) to remove moisture and then weighted (Sartorius Electronic Balance LA23OS with an accuracy of 10^{-4} g). This treatment was suitable for the removal of most of the water present initially in the polymer matrix as stated in a preceding work [8].

Sorption experiments were carried out at ambient temperature (25 ± 1 °C). Appropriate saturated salt slushes were used to provide constant water activities (a_w) ranging from 0.26 to 0.98 in accordance with standard UNE-EN ISO 483:1988. Ideal behaviour is assumed, whence activity is evaluated as the ratio between the pressure of the pure vapour [p] and the water vapour pressure at 25 °C [p_0] i.e: $a_w = p/p_0$. Beakers (100 ml) containing salt slushes were placed into 1-L air-tight glass jars. The PP/EVOH films were placed over beakers containing salt slushes. The samples were allowed to rehumidify for more than 4 weeks, at which time they had equilibrated with their surroundings, and then re-weighted. Moisture uptake at equilibrium was represented by percentage regain, defined as the moisture uptake (M_∞) per unit mass of the dry specimen (m_e) and the solubility coefficients (S) were calculated using the following equation:

$$S = \frac{M_\infty}{m_e p^o a_w} \quad (3)$$

where p^o is the saturation vapour pressure at 25 °C [2].

2.2.3. FTIR

Fourier transform infrared spectroscopy (FTIR) was performed in the transmission mode with an OPUS/IR PS15 spectrometer (Bruker). The spectra were the results of 32 coadded interferograms at 2 cm^{-1} resolution between 400 and 4000 cm^{-1} with collection times of approximately 1 min. Owing to the relatively low polarity of the samples, this time is short enough to prevent any significant change in moisture content during FTIR measurement. In fact, sealing of the samples against the atmosphere was not needed to obtain reproducible results. The intensity of the peak at 1167 cm^{-1}, characteristic for methyl group wagging in PP, was taken as the internal standard to normalize the entire spectrum. The amount of sorbed moisture was detected as the difference between the hydrated spectrum and the spectrum of anhydrous specimen. The integrated areas of the water sensitive bands as a function of time were used to calculate the water diffusion coefficients (D). Tests were performed on the same samples used for water uptake and solubility coefficient calculations.

From another point of view, the relationship between the plasticization factor and the decrease in the absorbance of the polymer bands can be inferred from the linear relationship between absorbance and concentration postulated in the Beer–Lambert law. If linearity is kept, the equation proposed by Baschetti et al. [15] will provide the plasticization factor of the EVOH fraction:

$$\%\ \text{plasticization} = \frac{\Delta V}{V_0} = -\frac{\Delta A}{A_0} \quad (4)$$

where ΔA and ΔV represent, respectively, the changes in the area of the band and the changes in the volume of the sample, while A_0 and V_0 are their initial values.

More detailed analysis of the IR spectra has been achieved by fitting the overall band profiles of the water ν_{OH} stretching bands. The band decomposition of the water FTIR spectra has been performed on the basis of the four-state model, which takes into account the four IR bands usually observed for water ν_{OH} vibration, and has been explained in preceding papers [8,16,17]. Furthermore, the time evolution of the water structure has been completed by independently examining the sorption dynamics for each component area of the ν_{OH} water band. The area of each Gaussian component as a function of hydration time has been fitted with single-exponential curves and the relaxation times were determined by using Eq. (5):

$$A = A_0[1 - \exp(-t/\tau)] \quad (5)$$

where A is the area for each component, A_0 is the maximal area, and τ is the relaxation time [18].

3. Theoretical background

3.1. Analysis of water clustering

Zimm and Lundberg [19,20] have developed a method which analyses water clustering from the single shape of the experimental

isotherm. They defined a clustering function $G_{11}/\bar{v}_1$ considering the statistical molecular distribution in a binary (1–2) component system and γ_1, the volume fraction activity coefficient of component 1 (water).

$$\frac{G_{11}}{\bar{v}_1} = -\phi_2\left[\frac{\partial(a_1/\phi_1)}{\partial a_1}\right]_{p,T} - 1 \tag{6}$$

where $\gamma_1 = a_1/\phi_1$, a_1 and ϕ_1 are, respectively, the activity and the volume fraction of component 1, ϕ_2 the volume fraction of component 2 (polymer), with $\phi_2 = 1 - \phi_1$. The analysis assumes that the polymer and water bulk add up. The clustering function $G_{11}/\bar{v}_1$ is easily computable from the water sorption isotherms. The average number of solvent molecules in a cluster or cluster number (MCS) can be evaluated by

$$\mathrm{MCS} = 1 + \left[\frac{\phi_1 G_{11}}{\bar{v}_1}\right] \tag{7}$$

3.2. Modelling diffusion data

The diffusion of water in thin layer films of thickness L is assumed to follow Fick's second law. A widely used approximation is that at short times (up to $M_t/M_\infty = 0.5$), the amount of substance diffused is proportional to t^n [21] and is given by.

$$\frac{M_t}{M_\infty} = \frac{4}{L}\left(\frac{Dt}{\pi}\right)^n \tag{8}$$

The FTIR technique does not directly give the mass of diffusant at a given depth, but provides absorbance (A_t and A_∞) data, which are proportional to the instantaneous mass of the diffusant (M_t and M_∞, respectively) by the Beer–Lambert law, so that Eq. (8) may be written as [1]:

$$\frac{A_t}{A_\infty} = \frac{4}{L}\left(\frac{Dt}{\pi}\right)^n \tag{9}$$

In Eqs. (8) and (9) the value of the exponent n depends on the mode of sorption. For a clear understanding of the diffusion mechanism, the sorption results have been further fitted to a relation of the type:

$$\frac{A_t}{A_\infty} = Kt^n \tag{10}$$

Normally, if the exponent $n = 0.5$ diffusion is termed as Fickian or Case I.

4. Results and discussion

4.1. Characterization of the structure of PP/EVOH blends

The micrographs published in a previous work showed that the blends are biphasic, and EVOH dispersed across the PP matrix [8]. The dispersed phase is spherical and the size of the dispersed structures increased with the EVOH concentration. The dispersed phase underwent debonding on fracture and no rests of the PP matrix were observed, showing a poor interfacial adhesion between the two phases. The microcavities in the interphase region between both components explain their lower density than predicted by Eq. (1). The void volume fractions, reported in Table 1, grow exponentially from 10 to 40% EVOH in the binary blends.

From another point of view, the degree of crystallinity of the iPP fraction estimated from the band ratio $A_{998}/_{973}$ for the 90/10 films remains roughly constant with respect to 100% iPP films, but significantly increases for EVOH contents ≥20%. These data are consistent with the fact that both the crystallization temperature of iPP, obtained in dynamic conditions, and the isothermal crystallization rate are significantly increased by the EVOH presence in the binary blends as a result of the induction effect of the EVOH crystallites, previously formed, on the crystal nucleation of iPP. In contrast, the crystallization behaviour of the EVOH copolymer is not modified by the presence of molten iPP, which is directly linked to the immiscibility of both components in the melt [22]. Therefore, the observed linear increase of the band ratio $A_{1145\ \mathrm{cm^{-1}}}/A_{1096\ \mathrm{cm^{-1}}}$ from 20% EVOH onwards is attributed to a modification in the distribution and strength of both intra- and intermolecular interactions of EVOH within the greater spherical domains. This ratio has not been obtained for the 90/10 blend as the 1145 $\mathrm{cm^{-1}}$ band is undetectable.

Table 1
Comparison of experimental and theoretical densities and FTIR absorbance ratios in PP/EVOH films as function of blend composition.

Blend composition	Experimental density (g/cm^3)	Predicted density	Void volume fraction	$A_{998/973}$	$A_{1145/1096}$
100/0	0.899 ± 0.001	0.899	0	0.85 ± 0.01	–
90/10	0.918 ± 0.004	0.921	0.0031	0.83 ± 0.02	–
80/20	0.936 ± 0.003	0.944	0.0083	0.94 ± 0.01	0.32 ± 0.042
70/30	0.949 ± 0.002	0.968	0.0196	0.89 ± 0.03	0.41 ± 0.053
60/40	0.983 ± 0.001	1.040	0.0550	0.96 ± 0.03	0.49 ± 0.02

In summary, on the one hand, from the density data and SEM images the free volume increases with EVOH content as a result of the poor interfacial adhesion. On the other hand, the degrees of crystallinity within both phases rise with EVOH concentration. Therefore, both effects balance to determine the transport properties in the binary blends.

4.2. Water sorption

Fig. 1 exhibits the water sorption isotherms of all the PP/EVOH blends studied in this work. The four isotherms have a similar sigmoïdal shape. At low water activities, the concavity of the isotherm with respect to the activity axis is attributed to dual-mode sorption, made up of Henry's and Langmuir's component. The first one is the illustration of random water absorption in the polymer matrix. The second one occurs when special adsorption sites are present in the polymer. In the PP/EVOH system, the Langmuir's component is a combination of two kinds of sorption: microvoids and hydroxyl groups establishing strong hydrogen bonding with water molecules.

At high activities, the isotherm upturns. The convex part is generally attributed to two phenomena according to the flexibility

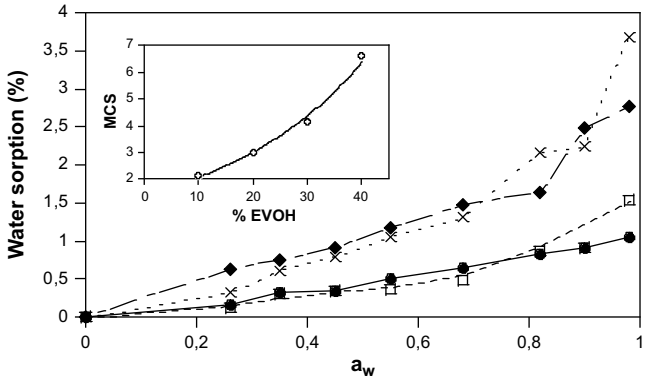

Fig. 1. Sorption isotherm of PP/EVOH blends in terms of water sorbed amount as a function of EVOH content at 25 °C. Legend: (●) 90/10; (□) 80/20; (◆) 70/30; (×) 60/40. Inset shows the average cluster number (MCS) vs. EVOH content.

of the matrix and its affinity for water, plasticization (highly hydrophilic) or clustering (hydrophobic) [23]. Opposite to EVOH copolymers [2,4] as the hydrophobicity of the PP phase limits the polymer from swelling, water clustering around the hydrophilic sites is the more likely mechanism for the upper part of the isotherm, although plasticization also plays a minor role in high EVOH content films at $a_w \geq 0.90$.

Regarding EVOH content, the differences in water uptakes between the 90/10 and 80/20 on the one hand, and 70/30 and 60/40 on the other, are only strongly accentuated as the water activity rises. The reason why the blends do not show clearly ranked differences in water uptake at low water activities lies in the blends' morphology. Plasticization being negligible in this regime, as will be confirmed in the following section, the water uptake is the result of the balance between the number of hydrophilic sites and the existing free volume. As the interfacial voids are greater in 80/20 than 90/10 and in 60/40 with respect to 70/30, the only possible explanation to this behaviour is the difference in the degree of crystallinity within both phases which rises with EVOH concentration.

The limit clustering activity values, calculated when MCS (Eq. (7)) are equal to 1, are 0.68, 0.60, 0.52 and 0.53 for 10, 20, 30 and 40% EVOH, respectively. These results are in agreement with the points of inflection in the isotherms of Fig. 1 at which the dual-mode sorption theory no longer applies. The cluster numbers (MCS), presented in Fig. 1 as an inset, rise exponentially with increasing blend hydrophilicity. On the other hand, except for the 90/10 films the average clusters' size for the PP/EVOH blends is higher than the size estimated for an EVOH copolymer of the same ethylene content [2]. This fact is a consequence of the different mechanism of water sorption between PP/EVOH blends and pure EVOH at mid and high water activities. As a result of the strong plasticizing effect in the latter, subsequent molecules sorb at the increasing number of newly available polar sites, thus, limiting the average cluster size around the hydroxyl groups [24], estimated by the Zimm Lundberg theory. Nonetheless, as hydration continuous and beyond a certain water content the opened volume allows the formation of water-rich domains or "bulk water", that is to say, water aggregates of fully coordinated water molecules not bound to the polymer [25,26]. Bulk water, as detected by IR spectroscopy, is water showing a band profile similar to liquid water with a broad OH stretching band with its maximum at 3400 cm^{-1} [8], as it is seen in pure EVOH difference FTIR spectrum [4].

4.3. Solubility coefficients and plasticization factors

The water solubility coefficients (S) of the PP/EVOH films at 0.98 water activity, calculated using Eq. (3), are shown in Fig. 2. The values for pure PP and EVOH have been included for comparison. As expected, the % water uptake and water solubility increase linearly with EVOH content, owing to the increasing number of OH groups within the polymer matrix able to develop strong hydrogen bonds with the water molecules.

From another point of view, FTIR spectroscopy is capable of determining structural changes in the polymer matrix upon water sorption. Apart from the water sensitive bands, the only significant change observed in the PP/EVOH spectra concerned the EVOH fraction and is the gradual decrease of the broad envelope centred at 1092 cm^{-1}, which hides the contribution of at least an amorphous band at 1115 cm^{-1}. On the other hand, the characteristic crystallinity peak at 1145 cm^{-1} [27] does not modify its intensity. Unsurprisingly, water molecules mainly concentrate in the amorphous EVOH fraction intercepting inter- and intramolecular hydrogen bonding provided by the hydroxyl groups and incrementing the polymer free volume [28].

The plasticization factors were determined by introducing in Eq. (4) the area of the band centred at 1092 cm^{-1} for dry and water-saturated films. The values obtained at 0.98 water activity are summarized in Fig. 2. The degree of plasticization increases linearly with EVOH content up to 30%, but tends to stabilize for the highest concentration. Moreover, even in the latter blends this parameter is significantly smaller than that of EVOH copolymer [6]. This is due to the confinement of the EVOH phase in isolated spherical domains within the hydrophobic PP phase, which slows down the EVOH fraction from swelling.

Table 2 displays the water solubility coefficients (S) and plasticization factors of 90/10 and 70/30 PP/EVOH blends as a function of water activity. As expected from the sorption isotherms, the coefficients for the 80/20 and 60/40 films are coincident within experimental error with those of 90/10 and 70/30 compositions, have been omitted for the sake of brevity. The solubility coefficients respectively, except at high water activities. Therefore, their values for the 90/10 PP/EVOH blends are roughly constant over the entire activity range, whereas for the 80/20, 70/30 and 60/40 films they remain constant up to 0.90, 0.82 and 0.68, respectively, but exhibit statistically significant greater values from there onwards. The invariance of the solubility indicates that over the aforementioned water activity range, the observed degree of plasticization is too small to affect macroscopic properties. On the contrary, the solubility coefficients of water in pure EVOH increased exponentially with increasing a_w, as a result of the strong plasticization effect of sorbed water [2].

4.4. Diffusion data

Water molecules sorbed into PP/EVOH films are identified in the vibrational spectrum by means of an increase in absorbance, compared to the dry polymer, at specific regions. The vibrations responsible for these changes, seen in Fig. 3, are the fundamental stretching (ν_{OH}) between 3700 and 3000 cm^{-1}; the 2150 cm^{-1} band

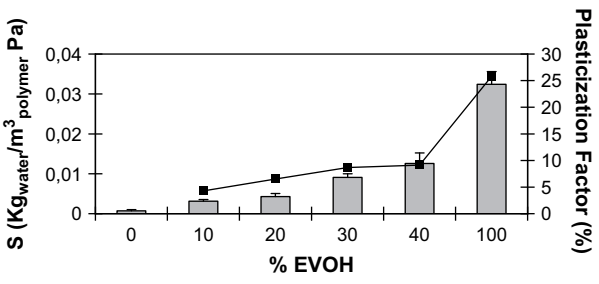

Fig. 2. Water solubility coefficients (S) (bars) and plasticization factors (lines) of the EVOH amorphous fraction in PP/EVOH films at 25 °C and 0.98 water activity.

Table 2
Water solubility coefficients (S) and plasticization factors of the EVOH amorphous fraction in 90/10 and 70/30 PP/EVOH films at 25 °C vs. water activity (a_w).

a_w	10% EVOH		30% EVOH	
	$S \times 10^3$ ($kg_{water}/m^3_{polymer}$ Pa)	Plasticization factor (%)	$S \times 10^3$ ($kg_{water}/m^3_{polymer}$ Pa)	Plasticization factor (%)
0.26	1.90 ± 0.34	–	7.26 ± 0.30	0.84 ± 0.55
0.35	2.76 ± 0.42	2.22 ± 0.40	6.64 ± 1.55	2.72 ± 0.28
0.45	2.17 ± 0.12	3.18 ± 0.19	6.03 ± 1.30	3.75 ± 0.82
0.55	2.66 ± 0.41	4.23 ± 0.37	6.44 ± 0.86	4.76 ± 0.52
0.68	2.76 ± 0.56	4.47 ± 0.55	6.48 ± 0.38	6.01 ± 0.83
0.82	2.76 ± 0.73	4.74 ± 0.80	6.00 ± 0.42	7.09 ± 0.43
0.9	2.69 ± 0.53	5.15 ± 0.48	8.30 ± 1.0	7.28 ± 0.34
0.98	3.15 ± 0.42	4.28 ± 0.87	9.10 ± 0.9	8.69 ± 0.69

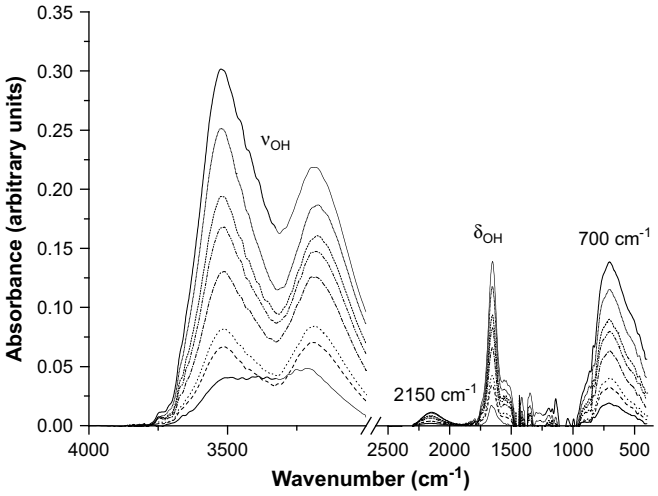

Fig. 3. Subtraction FTIR spectra collected at different sorption times in the case of water vapour sorption test at $a_w = 0.98$ in a 70/30 PP/EVOH film.

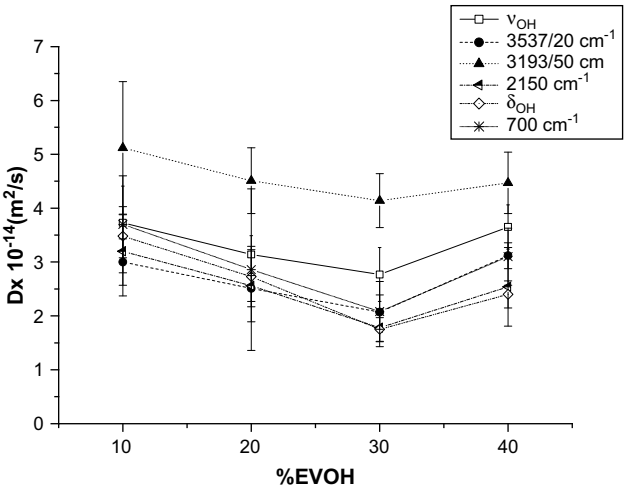

Fig. 5. Diffusion coefficients for water vapour at 25 °C and 0.98 water activity in PP/EVOH films as a function of EVOH content.

assigned to vibrations from the scission and rocking of water; the water OH in-plane bending vibration (δ_{OH}) at 1652 cm^{-1} and the 700 cm^{-1} band arising from the out of plane vibrations of O–H groups or librations. The fundamental OH stretching vibration is divided into two peaks. The one in the higher frequency region, around 3520–3530 cm^{-1}, has been assigned to unassociated water, dimers and loosely bound water. The peak in the lower frequency region is associated with water bound by strong hydrogen bonds to the polar groups of the polymer [8].

Sorption curves were plotted as percent absorbance gain of the water bending band (δ_{OH}) vs. square root of time for PP/EVOH films of increasing EVOH content at $a_w = 0.98$ (Fig. 4). The linear shape of the curves up to 50–60% maximal sorption levels indicated that the processes can be described as Fickian. Furthermore, from least-squares analysis of the data using Eq. (10), the n values for the four water bands were approximately 0.5, corroborating Fickian diffusion, independently of EVOH content and water activity.

The diffusion coefficient (D) was assumed to be independent of the concentration of the penetrant and Eq. (9) used to calculate the mean diffusion coefficient. Fig. 5 gathers the D values of the main water bands and the two peaks that form the fundamental OH stretching vibration, as function of EVOH content at $a_w = 0.98$. A first look reveals that the D values diminish linearly from 10 to 30% EVOH. Nevertheless, except for the bending band, these differences lie within the experimental error (ANOVA $P < 5\%$), which is mainly due to the difficulty to obtain reproducible film thickness and the non-uniform composition profile within each sample. Secondly, the coincidence of the D values of the 2150 cm^{-1}, δ_{OH} and 700 cm^{-1} peaks could allow the use of any of them to determine diffusion (ANOVA, $P < 5\%$). However, the best candidate is the bending vibration, because the errors associated with it are smaller. The reason lies in the fact that this band does not overlap with the polymer signals and does not shift over the entire sorption process [5–7]. Therefore, we will mainly refer to the bending band from now on.

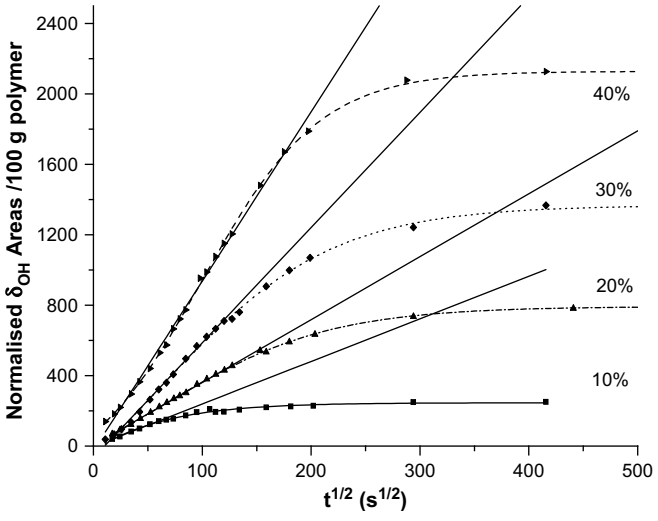

Fig. 4. FTIR water sorption curves for PP/EVOH films of increasing EVOH content at 25 °C and 0.98 water activity.

Concerning the fundamental stretching region, the diffusion coefficients of the 3190 cm^{-1} peak are approximately twice the values of the higher frequency band in the four compositions studied. Moreover, the D values of the latter are in agreement with those of the other water bands, supporting the idea that the global diffusion process at high water activity is governed by the diffusion of loosely bound water and that the different types of water are absorbed at a different rate.

From another point of view, the bending band diffusion coefficients for PP/EVOH 90/10 and 70/30 films are presented in Fig. 6 as a function of water activity, together with data found in literature for EVOH copolymer of the same ethylene grade [4].

In relation to PP/EVOH 90/10 films, the diffusion coefficients decrease exponentially with water activity, reaching a constant value at $a_w = 0.82$ ($r^2 = 0.998$). The same trend is observed for 70/30 films but the transition occurs at a lower water activity, 0.55–0.68 ($r^2 = 0.990$). Moreover, 70/30 films display significantly lower values than 90/10 blends (Student's t-test, $P < 0.05$) in the whole activity range. Similar results have been encountered for the other water bands.

Opposite to inert gases, marked decreases of the diffusion coefficients with water vapour concentration have been observed in several polymers. This is a consequence of the strong localized interactions developed between the water molecules and polar groups in the polymer [29,30]. Accordingly, the decrease of the D values with water activity is a consequence of the "sticking" of the first water molecules at the OH groups of the EVOH forming the

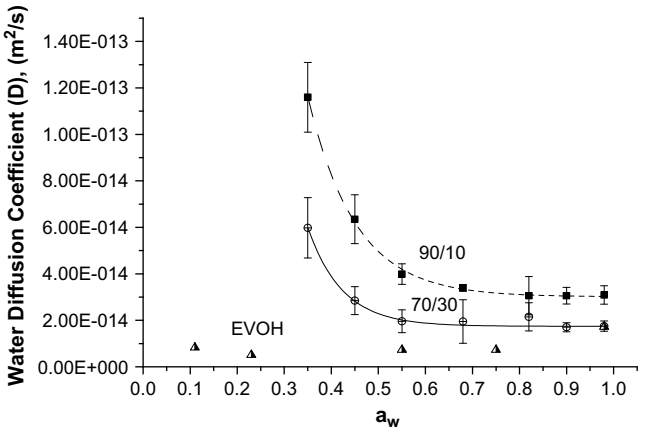

Fig. 6. Bending band diffusion coefficients of PP/EVOH 90/10 and 70/30 films compared with those found in literature for pure EVOH [4].

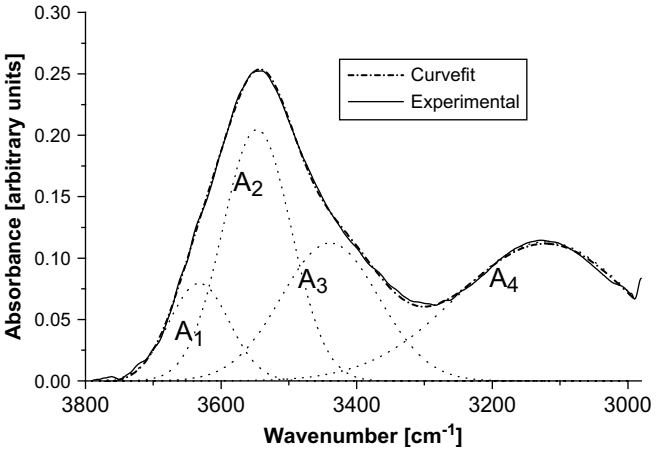

Fig. 7. Curve fitting analysis of the difference spectrum corresponding to water vapour sorbed at equilibrium ($a_w = 0.98$, 25 °C) in a 70/30 PP/EVOH film. The figure displays the experimental line shape, the simulated profile and the four resolved components.

first hydration layer, and of the further aggregation in small clusters around these sites to constitute the effective hydration region [8]. Besides, the observed plasticization in 90/10 and 70/30 blend films is too small to affect diffusion as the coefficients reach a minimum at the high activity range. Furthermore, the higher number of interacting sites and the greater clusters size contribute to a further reduction of the effective diffusivity on increasing EVOH content from 10 to 30% at $a_w = 0.98$. The consequences are lower D values and higher dependence on water concentration [31]. Nevertheless, this factor alone does not explain the slightly different behaviour of the 40% EVOH sample (Fig. 5). A contribution to this observation could come from a higher degree of plasticization, but this is not seen by FTIR. Thus, this effect is attributed to the greater void space around EVOH spheres, which makes the plasticized interface a preferential pathway for moisture diffusion.

Regarding pure EVOH, diffusion coefficients are at least one order of magnitude smaller with respect to 70/30 PP/EVOH blends at low water activities. The reasons are the faster free volume blocking, due to the superior number of hydrophilic sites, and differences in initial free volume owing to the high inter- and intrachain self-association in EVOH copolymers. It is worth mentioning, that D data appeared to be the lowest not at 0.11 but at 0.23 water activity (Fig. 6). These results are in accordance with the presence of a Langmuir contribution in this range observed in the sorption isotherms and oxygen permeability values before plasticization took place [4,6]. Otherwise, as a result of an exponential increase above $a_w = 0.54$, the D values become super imposable with those of the 70/30 blends at very high water activities. This is due to the well-known plasticization process undergone by EVOH copolymers in this regime of water activity.

4.5. Water–polymer interactions

Attempts have been made to solve the time dependency of the water structure in the PP/EVOH blends at 0.98 water activity. Band decomposition of water FTIR spectra has been performed on the basis of the four-state model, which takes into account the bands observed for liquid water ν_{OH} vibration [8]. Fig. 7 displays the water experimental subtraction spectrum along with its curve fitting analysis in a 70/30 PP/EVOH film at equilibrium. The spectrum exhibits four components. According to their positions from high to low wavenumber, they can be ranked from the strength of hydrogen bonding, i.e., band A_1, A_2, A_3 and A_4 reflecting very weak, weak, medium and strong hydrogen bonds, respectively.

Focusing on the relative distribution of the four types of water molecules shown in Fig. 8, it is clear that they are present in every blend composition at any water content, although their relative contributions vary in the time course of hydration. Thus, the A_4 band, which corresponds to fully hydrogen bonded water molecules directly attached to the active sites of the polymer (first hydration layer), is more pronounced in the early stages of exposure to water vapour. When the water content increases, its relative population is reduced to the benefit of the remaining components, the greatest relative raise corresponding to the A_3 band. This band has been assigned to fully hydrogen bonded species which form the second hydration layer or the clusters around the hydrophilic polymer sites. Besides, the A_1 and A_2 components reflect, respectively, the asymmetric and symmetric O–H stretching vibration of water monomers confined into excess free volume, and partially

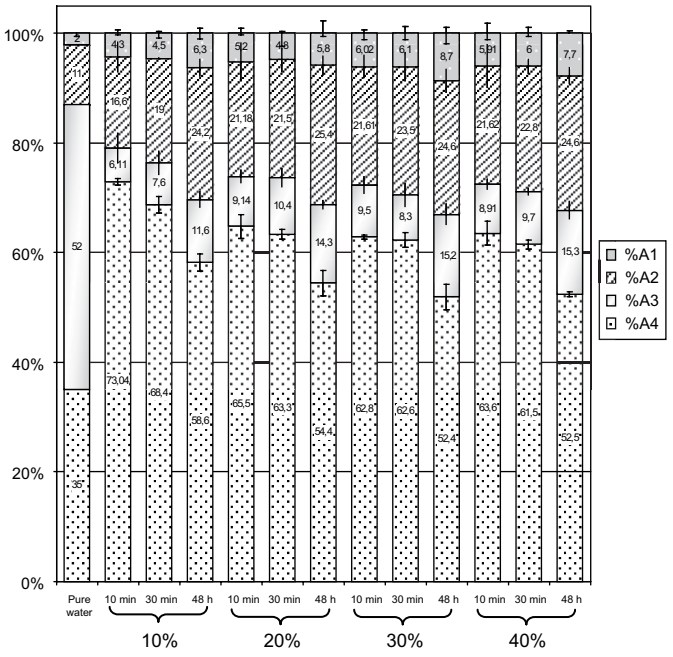

Fig. 8. Relative contributions of the four bands corresponding to ν_{OH} of pure water and water absorbed in PP/EVOH films of increasing EVOH content, at various stages of hydration at 0.98 water activity.

hydrogen bonded water molecules. The latter have one of their OH groups participating in hydrogen bonding to other water molecules, and may either form self-associated dimers or may be weakly bonded to the aforementioned clusters [8]. Moreover, there are significant differences in the relative contribution of both the A_4 band, which increases, and the A_3 component, which decreases, in the 90/10 blends in relation to the more hydrophilic mixtures, both in the "early" and the "late" stages of hydration (ANOVA, $P < 5\%$). These results are in accordance with the lower average cluster size estimated for the 90/10 films.

Besides, the alterations observed in the water structure are also evident on the average energy of the water H bonds. This is shown by large frequency shifts from the band positions and changes in band half widths. Table 3 presents the recovered parameters from band fitting FTIR corrected spectra of pure water [17] and water sorbed in the PP/EVOH films.

Interestingly, bands A_1 and A_2 in blends with EVOH content $\geq$20% experiment a similar trend, opposite to band A_4. They significantly upshift until equilibrium (blue shift), $\Delta\nu_0 \cong 30 \pm 10$ and $25 \pm 5\ cm^{-1}$, respectively. These changes in band wave numbers go along with a narrowing in band half widths of $\Delta\nu^{1/2} = -22 \pm 9$ and $-18 \pm 5\ cm^{-1}$, respectively. These results suggest a weakening in the mean H bond strength. On the contrary, the A_4 component downshifts, $\Delta\nu_0 = -30 \pm 10\ cm^{-1}$, and this red shift goes along with a significant band broadening of $\Delta\nu^{1/2} = 30 \pm 4\ cm^{-1}$. Hence, the average H-bonding strength and the distribution of H bonds of the primarily hydrating water progressively grow since the early steps of hydration until saturation. Finally, band A_3 behaviour is more difficult to explain, since it displays a blue shift of $\Delta\nu_0 = 23 \pm 3\ cm^{-1}$ which is paralleled with the widening of the band, $\Delta\nu^{1/2} = 30 \pm 7\ cm^{-1}$. However, the dynamic exchange between sites and hydration layers may account for this band widening [25].

Again, there are differences with respect to the 90/10 films; the first three components exhibit blue shifts which go along with band width enlargements. Conversely, the A_4 band wave number (υ_0) remains unaltered within experimental error, although the band half width ($\Delta\nu^{1/2}$) experiments a large band narrowing ($\Delta\nu^{1/2} \cong 43\ cm^{-1}$). The latter result suggests that strong matrix–water H-bonding occurs in the early steps of hydration which weaken at later stages.

Another complementary approach to this analysis is to independently examine the dynamics of water sorption of each component area of the ν_{OH} band. The relaxation times (τ) (Eq. (5)) provide information about the sequential order of the intensity changes observed in the difference spectra [18]. The τ values for components 1–4 in 90/10 films were 69 ± 15, 131 ± 10, 165 ± 80 and 86 ± 14 min, respectively; whereas, for the same components in 70/30 blends were 360 ± 93, 318 ± 13, 435 ± 95 and 261 ± 16 min, respectively. Consequently, the motion sequential order in 90/10 films is $A_1 \rightarrow A_4 \rightarrow A_2 \rightarrow A_3$. Conversely, in 70/30 blends not only diffusion is slower but the sequential order changes to $A_4 \rightarrow A_2 \rightarrow A_1 \rightarrow A_3$. Besides, both the τ values and sequential motion of the intensity changes for 80/20 and 60/40 films are basically similar to those estimated for 70/30 blends.

From another point of view, the water spectra in the 3800–3000 cm^{-1} region collected at equilibrium at 7 different water activities reveal that as the activity increases, the experimental band around 3500 cm^{-1} becomes more and more significant in relation with the band at 3190–3150 cm^{-1} (Fig. 9). Analogous behaviours have been described in a wide variety of polymers [4,16,32].

This effect is further evidenced by plotting the results of the curve fitting analysis as a function of water activity in 90/10 and 70/30 films. Fig. 10a and b shows how the relative amount of A_4 water molecules gradually decreases with activity, while those of the $A_1 + A_2$ components increase. Although the general trend is similar in the two blends, the rate of these variations depends on the film composition. Both plots show a point of inflection occurring at approximately 0.55 water activity for 70/30 films and above 0.82 for 90/10 blends. In addition, A_3 water molecules remain constant, within experimental error, until $a_w = 0.98$ in both compositions; the A_3 population is then increased by 1.6 and 1.4 factors for 70/30 and 90/10 films, respectively.

Furthermore, the A_1, A_2 and A_3 components in 90/10 films display blue shifts of $\Delta\nu_0 \cong 19$, 17 and 15 cm^{-1}, respectively, from 0.82 activity onwards; similarly, the A_2 and A_3 peaks in 70/30 blends exhibit blue shifts of, $\Delta\nu_0 \cong 9$ and 20 cm^{-1}, respectively, from 0.55 water activity onwards. Thus, there is a decrease in the average hydrogen bonding strength of the water species of the second hydration layer at equilibrium as the activity increases, despite the raise in their relative population. In 70/30 films, these changes are coincident with the clustering limit activity. On the whole, the evolution of the relative population of interacting water species at equilibrium with water activity is basically similar to the trend observed upon hydration time at $a_w = 0.98$, in both compositions.

In summary, the described findings are consistent with the physical picture of a system where the hydrogen bonding structure

Table 3
Summary of A: band positions (ν_0, cm^{-1}) and B: band widths ($\Delta\nu^{1/2}$, cm^{-1}) for water ν_{OH} stretching modes in pure water and in PP/EVOH films as a function of EVOH content at 0.98 water activity and 25 °C.[a]

Band	Pure water	10%	20%	30%	40%
		30 min/48 h	30 min/48 h	30 min/48 h	30 min/48 h
A: band positions					
A1	3630	3583/3621	3610/3641	3610/3628	3605/3634
A2	3550	3505/3526	3522/3546	3521/3541	3522/3549
A3	3400	3395/3410	3403/3424	3400/3423	3406/3432
A4	3232	3179/3186	3162/3141	3184/3142	3162/3128
B: band widths					
A1	80	107/146	126/113	150/118	131/112
A2	155	133/146	147/134	148/125	138/125
A3	213	115/142	133/157	118/153	126/163
A4	205	430/387	357/378	322/349	325/358

[a] For each blend, three spectra have been fitted which correspond to "early" and "late stages of hydration", respectively and the averages calculated. Typical confidence intervals are $\pm 5\ cm^{-1}$ for band positions and widths, although the intervals may be twice to thrice for the A4 band.

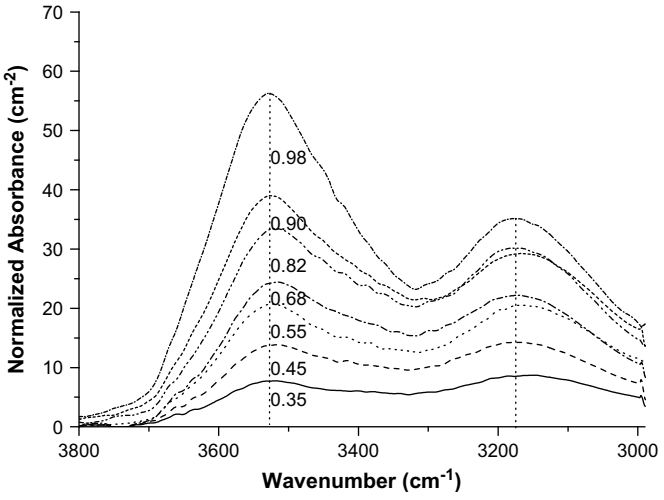

Fig. 9. Subtraction FTIR spectra in the 3800–2700 range (ν_{OH} band) corresponding to water absorbed at equilibrium at different a_w in 70/30 PP/EVOH films.

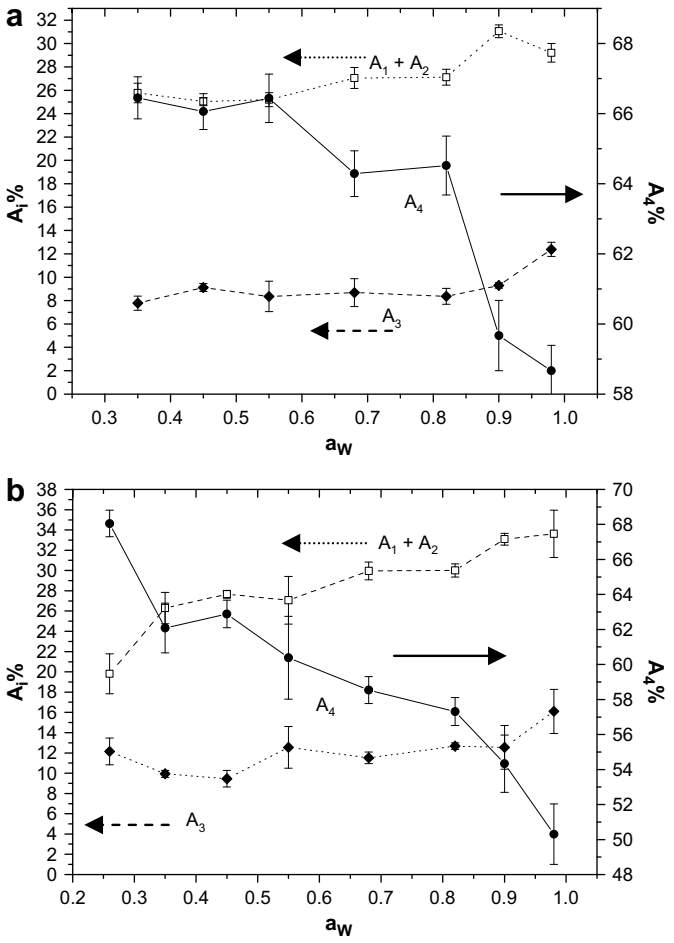

Fig. 10. Relative absorbance area of the different components of the subtraction spectra collected at water vapour sorption equilibrium, reported as a function of water vapour activities. a: PP/EVOH 90/10; b: PP/EVOH 70/30.

of water changes as a function of hydration time and external water activity. In fact, *at very low hydration times* and *low activities* strong interactions with the OH groups of the EVOH fraction are more likely to develop for enthalpic reasons [16]. Nonetheless, the bands A_1, A_2 and A_3 are also present in the polymer; therefore, the second hydration layer, with both strong and weak interactions, can be formed on certain sites before all accessible polar groups are saturated. As the *water content increases*, reachable interacting sites get closer to saturation and weak interactions play an increasingly significant role. Apart from this, the stretching modes of A_1, A_2 and A_3 molecules shift in the direction of weaker bonding, in spite of the rising in their relative population. It is likely that by successively adding water the size of the clusters around interacting sites increases, but their shape does not allow the formation of strong hydrogen bonds [32].

Moreover, the mean H-bonding strengths of A_1, A_2 and A_3 water species are larger in 90/10 films in comparison with the more hydrophilic mixtures. Thus, it is reasonably assumed that, although smaller in size, the shape of the clusters permits the formation of stronger hydrogen bonds. In contrast, the frequency of the A_4 band and its narrowing in 90/10 films suggest a decrease in the average hydrogen bonding strength upon hydration, whereas it keeps growing until equilibrium in blends with higher EVOH content. The obvious inference from this finding is that the water structure does not strictly correlate with the amount of sorbed water in the polymer [33].

From the assignment and time evolution of the components of the water ν_{OH} band, the processes of water adsorption followed by penetration into the 90/10 polymer film could be as follows: (1) monomeric water first adsorbs onto the polymer surface and partially diffuses into free volume because the value of component 1 is the smallest, (2) subsequent molecules penetrate and bind to the OH groups of the EVOH chain, (3) then weakly bonded dimers/trimers, which are molecularly dispersed in the polymer matrix, are formed and/or new water molecules bind with only one of its H atoms to the first hydration layer; finally (4), the aggregation of water molecules in small clusters around the polymer hydrophilic sites is completed, because the τ of component 3 is the largest. Since in PP/EVOH blends with EVOH content $\geq$20%, the τ value for component 1 is larger than those for components 4 and 2, the water forming stronger hydrogen bonding with hydrophilic polymer sites might be produced prior to water diffused into microvoids. Alike for the 90/10 blends, formation of fully hydrogen bonded clusters, around the polymer polar sites, should be the last step in the hydration process.

As a final point, the differences found between 90/10 films and blends with higher EVOH content are to be attributed to the specific morphology of the formers [34]. The lower degree of crystallinity in 90/10 blends together with the smaller void space around the EVOH spheres, explain the fact that monomeric water molecules diffuse into the PP fraction prior to binding the EVOH hydroxyl groups; while for films with EVOH content $\geq$20%, which have increasing gaps at the interphase with available sites for water molecules interaction, the sequence is the opposite.

5. Conclusions

FTIR along with gravimetric analysis has provided the following new information about the kinetics and interactions relevant to water sorption in PP/EVOH blends. The results would be useful to design suitable formulations for the food packaging industry with the best cost/properties ratio.

The sigmoïdal shape of the water sorption isotherms proves the existence of two mechanisms, below (dual-mode) and above a critical concentration value close the clustering limit activity. Plasticization being negligible at low water activities, the blends do not show clearly ranked differences in water uptake due to the complex blend morphology. Otherwise, at very high water activities the water content increases linearly and the average clusters' size rises exponentially with EVOH content.

Fickian sorption has been observed independently of the EVOH content or water activity at 25 °C. Diffusivity decreased linearly upon raising EVOH from 10 to 30% at 0.98 water activity, but reduced exponentially with water activity reaching a constant value. On the contrary, the solubility coefficients remained roughly constant at low and medium water activities. These behaviours have been attributed to a free-volume blocking regime as a consequence of the strong physico-chemical affinities of the water molecule for the polar sites of the amorphous EVOH fraction, in the absence of a significant moisture induced plasticization. The low plasticization is due to the confinement of the isolated EVOH spheres within the hydrophobic PP matrix.

In terms of water–polymer interactions, there is a distribution of water molecules with different hydrogen bonding strength which changes upon hydration time and water activity. Regardless of the EVOH content, the molecules more strongly associated by hydrogen bonding are dominant at low sorption levels, whereas those less hydrogen bonded prevail at high sorption levels. The main changes in water structure take place from the clustering limit activity onwards.

Besides, significant differences both in diffusion sequence of free/bound water and water structure, irrespective of hydration time and water activity, have been found between 90/10 films and blends

with higher EVOH content. As there are no differences, within experimental error, among the blends with 20, 30 and 40% EVOH, the dynamic sorption behaviour and state of water is not only proportional to the number of hydrophilic sites in the polymer network, but also dependent on the observed morphological differences.

Acknowledgements

Financial support for this work has been provided by Secretaría Xeral de Investigación e Desenrolo, Xunta de Galicia through grant XUGA-PGIDT02TMT17201PR.

References

[1] Cava D, Lagarón JM, López-Rubio A, Catalá R, Gavara R. Polymer Testing 2004;23:551–7.
[2] Zhang Z, Britt IJ, Tung MA. Journal of Polymer Science, Part B: Polymer Physics 1999;37:691–9.
[3] Lagarón JM, Giménez E, Saura JJ. Polymer International 2001;50:635–42.
[4] Cava D, Cabedo L, Gimenez E, Gavara R, Lagarón JM. Polymer Testing 2006;25:254–61.
[5] Döppers LM, Sammon C, Breen C, Yarwood J. Polymer 2006;47:2714–22.
[6] Cava D, Sammon C, Lagarón JM. Applied Spectroscopy 2006;60(12):1392–8.
[7] Cava D, Sammon C, Lagaron JM. Journal of Applied Polymer Science 2007;103:3431–7.
[8] Lasagabáster A, Abad MJ, Barral L, Ares A. European Polymer Journal 2006;42:3121–32.
[9] Abad MJ, Ares A, Barral L, Eguiazábal JI. Polymer International 2005;54:673–8.
[10] Ares A, Abad MJ, Barral L, García-Garabal S. E-Polymer, in press.
[11] Ares, A. Estudio de las propiedades barrera de filmes basados en polipropileno y copolímero de etileno y alcohol vinílico. Departamento de Física. E.U.P. Ferrol, PhD thesis, Universidad de A Coruña; 2006.
[12] Pehlivan H, Öxmihçi F, Tihminlioglu F, Balköse D, Ülkü S. Journal of Applied Polymer Science 2003;90:3069–75.
[13] Andreassen E. Infrared and Raman spectroscopy of polypropylene. In: Karger-Kocsis J, editor. Polypropylene: an A–Z reference. Dordrecht: Kluwer Publishers; 1999. p. 320–8.
[14] Sugiura K, Hashimoto M, Matsuzawa S, Yamura K. Journal of Applied Polymer Science 2001;82:1291–8.
[15] Baschetti MG, Piccinini TA, Barbari TA, Sarti GC. Macromolecules 2003; 36(25):9574–84.
[16] Cotugno S, Larobina D, Mensitieri G, Musto P, Ragosta G. Polymer 2001; 42:6431–8.
[17] Thouvenin M, Linossier I, Sire O, Péron JJ, Vallée-Réhel K. Macromolecules 2002;35:489–98.
[18] Ide M, Yoshikawa D, Maeda Y, Kitano H. Langmuir 1999;15:926–9.
[19] Zimm BH, Lundberg JL. Journal of Physical Chemistry 1968;60:425–8.
[20] Lundberg JL. Pure and Applied Chemistry 1972;31:261–81.
[21] Crank J. The mathematics of diffusion. 2nd ed. Oxford: Oxford Science Publications; 1975.
[22] Ares A, Marco C, Gómez M, Ellis G, Abad MJ, Barral L. European Polymer Journal, submitted for publication.
[23] Detallante V, Langevin D, Chappey C, Métayer M, Mercie R, Pinér M. Journal of Membrane Science 2001;190:227–41.
[24] Aucejo S, Marco C, Gavara R. Journal of Applied Polymer Science 1999;74:1201–6.
[25] Ping ZH, Nguyen QT, Chen SM, Zhou JQ, Ding YD. Polymer 2001;42: 8461–7.
[26] Karlsson GE, Gedde UW, Hedenqvist MS. Polymer 2004;45:3893–900.
[27] López-Rubio A, Lagarón JM, Giménez E, Cava D, Hernandez-Muñoz P, Yamamoto T, et al. Macromolecules 2003;36:9467–76.
[28] Hodge RM, Edward GH, Simon GP. Polymer 1996;37:1371–6.
[29] Karad S, Jones FR. Polymer 2005;46:2732–8.
[30] Morliére N, Valliéres C, Perrin L, Roizard D. Journal of Membrane Science 2006;270:123–31.
[31] Larobina D, Lavorgna M, Mensitieri G, Musto P, Vautrin A. Macromolecular Symposium 2007;247:11–20.
[32] Laporta M, Pegoraro M, Zanderighi L. Physical Chemistry Chemical Physics 1999;1:4619–28.
[33] Kitano H, Nagaoka K, Tada S, Gemmei-Ide M, Tanaka M. Macromolecular Bioscience 2008;8:77–85.
[34] Li L, Liu M, Li S. The Journal of Physical Chemistry B 2004;108:4601–6.